Appendix G
Underwater Noise Modelling of Impact Pile Driving
(Jasco - April 2017)

Underwater Noise Modelling of Impact Pile Driving

Based on a Preliminary Design of the Third Crossing of the Cataraqui River, Kingston, ON

Submitted to:

Phil Rouget
Golder Associates Ltd.
Contract: JASCO-002 / 1541774

Authors:

Zizheng Li
David Zeddies

21 April 2017

P001313
Document 01193
Version 2.0

JASCO Applied Sciences (Canada) Ltd
2305–4464 Markham Street
Victoria, BC V8Z 7X8 Canada
Tel: +1-250-483-3300
Fax: +1-250-483-3301
www.jasco.com

Suggested citation:

Li, Z. and D. Zeddies. 2017. Underwater Noise Modelling of Impact Pile Driving: Based on a Preliminary Design of the Third Crossing of the Cataraqui River, Kingston, ON. Document 01193, Version 2.0. Technical report by JASCO Applied Sciences for Golder Associates Ltd.

Disclaimer:

The results presented herein are relevant within the specific context described in this report. They could be misinterpreted if not considered in the light of all the information contained in this report. Accordingly, if information from this report is used in documents released to the public or to regulatory bodies, such documents must clearly cite the original report, which shall be made readily available to the recipients in integral and unedited form.

To comply with Accessibility for Ontarians with Disabilities Act, all italicized conventions, including Latin species' names, were removed.

Contents

Figures

Tables

Executive Summary

JASCO Applied Sciences Ltd, under contract to Golder Associates Ltd., performed an underwater acoustic modelling study of impact pile driving activities for constructing the Third Crossing over the Cataraqui River. Modelling was based on preliminary project designs provided by Golder Associated Ltd. This study assessed the impact pile driving noise to which fish, turtles, fish eggs, and fish larvae could be exposed. The modelling accounted for the acoustic emission characteristics of the driven pile by using a physical piling noise source model coupled to transmission loss model, which predicted the noise field. To predict the acoustic footprint associated with driving steel cylindrical pipe piles, the modelling considered the effects of pile driving equipment characteristics, bathymetry, water sound speed, and geoacoustic parameters. Due to shallow water depths and absorptive riverbed sediments, the distances to the thresholds based on Popper et al. (2014) were quite small. In this propagation environment—one where a significant portion of sound propagates through sediments—a bubble curtain mitigation system does not alter the threshold distances so is ineffective.

The results based on the dual criteria of Popper et al. (2014) are summarized below:

- The maximum distances to the thresholds for mortality or potential mortal injury to fish, turtles, fish eggs, and fish larvae were 3 m for peak pressure level (PK) and 6 m for the sound exposure level over 24 hours (SEL_{24h}).
- The maximum distances to thresholds for recoverable auditory injury to fish were 3 m for PK and 7 m for SEL_{24h}.
- Based on the qualitative thresholds of Popper et al. (2014), turtles are at high risk of recoverable injury within tens of metres of the pile, and fish eggs and larvae are at moderate risk of recoverable injury within this range; the relative risk drops to low for distances of hundreds to thousands of metres.
- The maximum distance to the SEL_{24h} threshold for temporary threshold shift (TTS, temporary loss of hearing sensitivity caused by excessive noise exposure) for fish was 86 m.
- Based on the qualitative thresholds of Popper et al. (2014), adult fish without a swim bladder or with a swim bladder not involved in hearing, as well as turtles, are at high risk of behavioural disruption within tens of metres of the pile. Fish with a swim bladder involved in hearing are at high risk within tens to hundreds of metres, and fish larvae are at only moderate risk of behavioural disturbance within tens of metres of the pile.

1. Introduction

The City of Kingston, ON, is proposing to address the area's growing transportation needs by constructing a bridge, known as the Third Crossing, that connects the east and west sides of the Cataraqui River. JASCO Applied Sciences Ltd (JASCO), under contract to Golder Associates Ltd. (Golder), performed an underwater acoustic modelling study to predict the underwater sound levels generated by impact pile driving during bridge construction based on a preliminary design. The goal of this study was to predict the extent of ensonification from pile driving and assess the potential effects on fish, turtles, fish eggs, and fish larvae from underwater noise, based on currently applied sound level thresholds for auditory injury and behavioural disturbance.

This study considered impact pile driving at one proposed location. JASCO's Pile Driving Source Model (PDSM) was used to simulate the sound radiating from the pile during impact pile driving. JASCO's Full Waveform Range-dependent Acoustic Model (FWRAM) was used to compute sound propagation for the defined scenario. FWRAM accepts the source signature, bathymetry, water sound speed profile, and riverbed geoacoustic parameters as inputs. Modelled results are presented in sound field isopleth maps and show the planar distribution of sound levels as a function of distance and direction from the pile. We used noise criteria thresholds for fish, turtles, fish eggs, and fish larvae proposed by Popper et al. (2014).

The following three subsections describe the modelled scenario, the species of interest, and the impact criteria applied to assess noise levels. Section 2 outlines how we estimated sound source levels, the sound propagation model used, and the procedure used to compute distances for a given threshold. Section 3 presents the modelled results in maps and tables. Section 4 interprets, discusses, and summarizes the results. A glossary of acoustic terminology is also included. Acoustic metrics, environmental parameters, information on sound and hearing for fish and turtles, and modelling approaches used in this study are presented in appendices.

1.1. Acoustic Modelling Scenario

Pier #4 was selected for modelling impact pile driving at the Third Crossing (Figure 1). It is located at 44°15.478′ N, 76°28.552′ W with a water depth of 0.54 m. This location has the thickest layer of sediment compared to other pier locations, might require more strikes to set into the bedrock, and is near the bird nesting protected wetland area to the north.

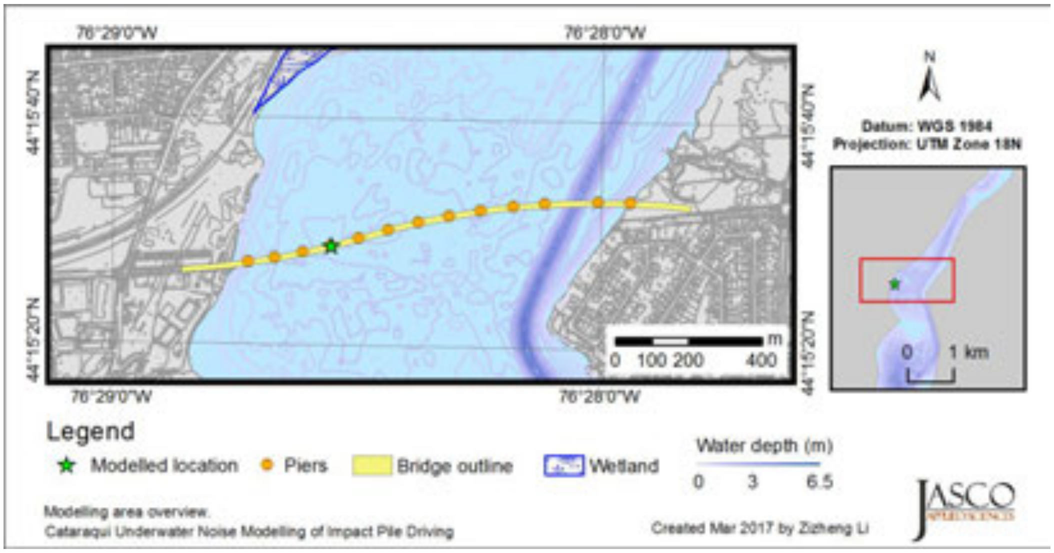

Figure 1. Study area overview showing the location of the model scenario at Pier #4 (Bowfin Environmental Consulting 2011). Bridge outline refers to Third Crossing.

1.2. Species of Interest

Using available literature, and conducting habitat assessment and fisheries inventories, Bowfin Environmental Consulting compiled the species known to occur or having the potential to occur in the project area (Bowfin Environmental Consulting 2011). The project task order (JASCO 002) includes a subset of these species, 24 species of fish (Table 1) and 5 species of turtle (Table 2), for consideration in this project.

Table 1. Fish species known to be present or having the potential to be present in the study area. Columns show the common name, scientific name, and hearing group where (I) is no swim bladder, (II) is swim bladder not involved in hearing, (III) is swim bladder involved in hearing, as proposed by Popper et al. (2014) (see Section 1.3 and Appendix C).

Common Name	Scientific Name	Hearing group	Common Name	Scientific Name	Hearing group
Alewife	Alosa pseudoharengus	III	Golden shiner	Notemigonus crysoleucas	II
American eel	Anguilla rostrata	II	Johnny darter	Etheostoma nigrum	II
Banded killifish	Fundulus diaphanus	III	Largemouth bass	Micropterus salmoides	II
Black crappie	Pomoxis nigromaculatus	II	Longnose gar	Lepisosteus osseus	II

Common Name	Scientific Name	Hearing group	Common Name	Scientific Name	Hearing group
Blackchin shiner	Notropis heterodon	III	Northern pike	Esox lucius	II
Blacknose shiner	Notropis heterolepis	III	Pugnose shiner	Notropis anogenus	III
Bluntnose minnow	Pimephales notatus	III	Pumpkinseed	Lepomis gibbosus	II
Brook silverside	Labidesthes sicculus	II	Rock bass	Ambloplites rupestris	II
Brown bullhead	Ameiurus nebulosus	III	Smallmouth bass	Micropterus dolomieu	II
Chinook salmon	Oncorhynchus tshawytscha	II	White sucker	Catostomus commersonii	III
Coho salmon	Oncorhynchus kisutch	II	Yellow bullhead	Ameiurus natalis	III
Common logperch	Percina caprodes	II	Yellow perch	Perca flavescens	II

Table 2. Turtle species known to present or having the potential to be present in the study area.

Common Name	Scientific Name
Blanding's turtle (Great Lakes/St. Lawrence population)	Emydoidea blandingii
Eastern musk turtle (stinkpot)	Sternotherus odoratus
Midland painted turtle	Chrysemys picta marginata
Northern map turtle	Graptemys geographica
Snapping turtle	Chelydra serpentina

1.3. Impact Criteria for Fish and Turtles

A recent working group, sponsored by the Acoustical Society of America and registered with the American National Standards Institute (ANSI) committee, published noise exposure criteria for fish and sea turtles (Popper et al. 2014). The working group published guidelines for a number of source types, including pile driving (Popper et al. 2014). The guidelines for injury use dual criteria, peak pressure level (PK) and sound exposure level over 24 hours (SEL_{24h}). Popper et al. (2014) do not present fixed thresholds for behavioural effects but instead assign relative risk levels for ranges from the source (near, intermediate, and far). While the relative distances do not correspond directly to specific distances, in general "near" might be considered to be in the tens of metres from the source, "intermediate" in the hundreds of metres, and "far" in the thousands of metres. Fish are classified based on their hearing capabilities, which are typically determined by whether a swim bladder is present and, if it is, whether it is directly involved in hearing (Appendix C.1).

The Working Group on the Effects of Sound on Fish and Turtles considered the available information about sea turtles and suggested similar criteria and thresholds for sea turtles as were suggested for fish. As with fish, Popper et al. (2014) do not define sound levels that may result in turtle behavioural response, but they assign relative risk levels based on ranges from the source (near, intermediate, and far). The turtles found near the project site are not sea turtles but no other criteria are available for turtles exposed to sound underwater so the Popper et al. (2014) criteria will be used. Table 3 summarizes the criteria used in this study to assess possible effects of pile driving sounds on fish and turtles.

Table 3. Thresholds for potential acoustic impacts on fish, turtles, fish eggs, and fish larvae, adapted from Popper et al. (2014). All criteria are presented as sound pressure even for fish without swim bladders (Fish I) because particle motion data do not exist. Relative risk (high, moderate, low) is given for animals at three distances from the source defined in relative terms as near (N), intermediate (I), and far (F). Fish I–No swim bladder; Fish II–Swim bladder not involved with hearing; Fish III–Swim bladder involved with hearing. PK–peak pressure level; SEL_{24h}–sound exposure level over 24 hours; TTS–temporary threshold shift.

Type of animal	Mortality and potential mortal injury		Recoverable injury		TTS	Masking	Behaviour
	SEL_{24h} (dB re 1 µPa²·s)	PK (dB re 1 µPa)	SEL_{24h} (dB re 1 µPa²·s)	PK (dB re 1 µPa)	SEL_{24h} (dB re 1 µPa²·s)		
Fish I	> 219	> 213	> 216	> 213	>> 186	(N) Moderate (I) Low (F) Low	(N) High (I) Moderate (F) Low
Fish II	210	> 207	203	> 207	>> 186	(N) Moderate (I) Low (F) Low	(N) High (I) Moderate (F) Low
Fish III	207	> 207	203	> 207	186	(N) High (I) High (F) Moderate	(N) High (I) High (F) Moderate

Type of animal	Mortality and potential mortal injury		Recoverable injury		TTS	Masking	Behaviour
	SEL_{24h} (dB re 1 µPa^2·s)	PK (dB re 1 µPa)	SEL_{24h} (dB re 1 µPa^2·s)	PK (dB re 1 µPa)	SEL_{24h} (dB re 1 µPa^2·s)		
Fish eggs and fish larvae	> 210	> 207	(N) Moderate (I) Low (F) Low		(N) Moderate (I) Low (F) Low	(N) Moderate (I) Low (F) Low	(N) Moderate (I) Low (F) Low
Turtles	210	> 207	(N) High (I) Low (F) Low		(N) High (I) Low (F) Low	(N) High (I) Moderate (F) Low	(N) High (I) Moderate (F) Low

2. Methods

2.1. Acoustic Source Parameters

The Third Crossing will be supported by steel cylindrical pipe piles, with a planned diameter of 1.067 m, length of 50 m, and wall thickness of 0.025 m. The impact hammer modelled was an APE D100-42 single acting diesel impact hammer with a 335 kJ maximum rated energy and a 10000 kg ram. For the purpose of the modelling, it was assumed that each pile would require 200 strikes (blow rate of 7 strikes/minute) to penetrate the sediments to a depth of 45 m to seat into bedrock. Within 24 hours, 16 piles are planned to be installed, resulting in 3200 strikes total. The project design provided by Golder Associated Ltd., including the equipment and operation plans associated with impact pile driving, is preliminary.

2.2. Impact Pile Driving Modelling Approach

The following three steps were applied to model sound levels from impact pile driving:

1. Sound radiating from the piles as they are driven into the sediment was modelled.
2. Propagation of sound through the water column and sediments was modelled as a function of range, depth, and azimuth.
3. The propagated sound field generated by the source and sound propagation models was used to compute received levels over a grid of simulated receivers, from which distances to criteria thresholds and maps of ensonified areas were generated.

Pile vibrations and corresponding source levels associated with impact driving of cylindrical piles were modelled using JASCO's Pile Driving Source Model (PDSM, Appendix D), a physical model of pile vibration and near-field sound radiation (MacGillivray 2014), in conjuction with the GRLWEAP 2010 wave equation model (GRLWEAP, Pile Dynamics 2010) to obtain an equivalent pile source signature consisting of a vertical array of discrete point sources. This signature accounts for several parameters that describe the operation: pile type, material, size, and length; the pile driving equipment; and approximate pile penetration rate. With the PDSM model, the amplitude and phase of the point sources along the array were computed so that they collectively mimicked the time-frequency characteristics of the acoustic wave at the pile wall that results from a hammer striking the top of the pile. This approach accurately estimates spectral levels within the band 10–1000 Hz where most of the energy from impact pile driving is concentrated. The acoustic energy at higher frequencies was estimated using an extrapolation method (Zykov et al. 2016) to extend modelled levels up to 4 kHz by applying a −2 dB per 1/3-octave-band roll-off coefficient to the SEL value starting at the 1000 Hz band.

JASCO's Full Waveform Range-dependent Acoustic Model (FWRAM, Appendix E) was used to determine received levels as a function of depth, range, and azimuth. FWRAM is a time-domain acoustic model that accepts as input a PDSM-generated array of point sources representing the pile and computes synthetic pressure waveforms via Fourier synthesis, from which several metrics—sound pressure level (SPL), peak pressure level (PK), and sound exposure level (SEL)—can be obtained. FWRAM applies a wide-angle parabolic equation (PE) solution to the acoustic wave equation (Collins 1993) based on a version of the U.S. Naval Research Laboratory's Range-dependent Acoustic Model (RAM) which has been modified to account for waterborne energy loss to shear waves in a solid seabed (Zhang and Tindle 1995). FWRAM takes environmental inputs including bathymetry, water sound speed profile, and riverbed geoacoustic profile (Appendix B). FWRAM was set to run for 24 radials with 15° azimuth angle spacing and 2 m range step for each radial.

SEL over 24 hours can be obtained using Equation A-4 with the parameter of 3200 strikes over 24 hours as described in Section 2.1, so per-strike values can be scaled by $10\times\log_{10}(3200)$ = 35.1 dB to obtain SEL_{24h}.

In this study, we also considered the potential for an unconfined bubble curtain mitigation system to impact the sound levels. Bubble curtain systems use manifold rings driven by air compressors to generate a cloud of bubbles around the pile. Noise mitigation is achieved by two mechanisms (Lucke et al. 2011): first, each bubble scatters sound because of the high acoustic impedance mismatch between the water and the injected air that forms the bubble; second, at certain wavelengths, acoustic waves cause bubbles to resonate, resulting in a net acoustic energy loss. The broadband attenuation level achieved depends on environmental factors, the characteristics of the pile, and the penetration depth of the pile into the substrate. Bubble curtains are less effective when a significant portion of sound travels unimpeded through the sediment substrate and enters the water column via the bottom interface at a distance greater than the bubble curtain can contain (WSDOT 2010), however.

2.3. Estimating Distances to Threshold Levels

Sound level contours and distances to specific sound levels were calculated based on the underwater sound fields predicted by the propagation models, sampled by taking the maximum value over all modelled depths above the river floor for each location in the modelled region. Two distances relative to the source are reported for each sound level: 1) R_{max}, the maximum range to the given sound level over all azimuths, and 2) $R_{95\%}$, the range to the given sound level after the 5% farthest points were excluded (see examples in Figure 2).

The $R_{95\%}$ is used because sound field footprints are often irregular in shape. In some cases, a sound level contour might have small protrusions or anomalous isolated fringes. This is demonstrated in the image in Figure 2(a). In cases such as this, where relatively few points are excluded in any given direction, R_{max} can misrepresent the area of the region exposed to such effects, and $R_{95\%}$ is considered more representative. In strongly asymmetric cases such as shown in Figure 2(b), on the other hand, $R_{95\%}$ neglects to account for significant protrusions in the footprint. In such cases R_{max} might better represent the region of effect in specific directions. Cases such as this are usually associated with bathymetric features affecting propagation. The difference between

R_{max} and $R_{95\%}$ depends on the source directivity and the non-uniformity of the acoustic environment.

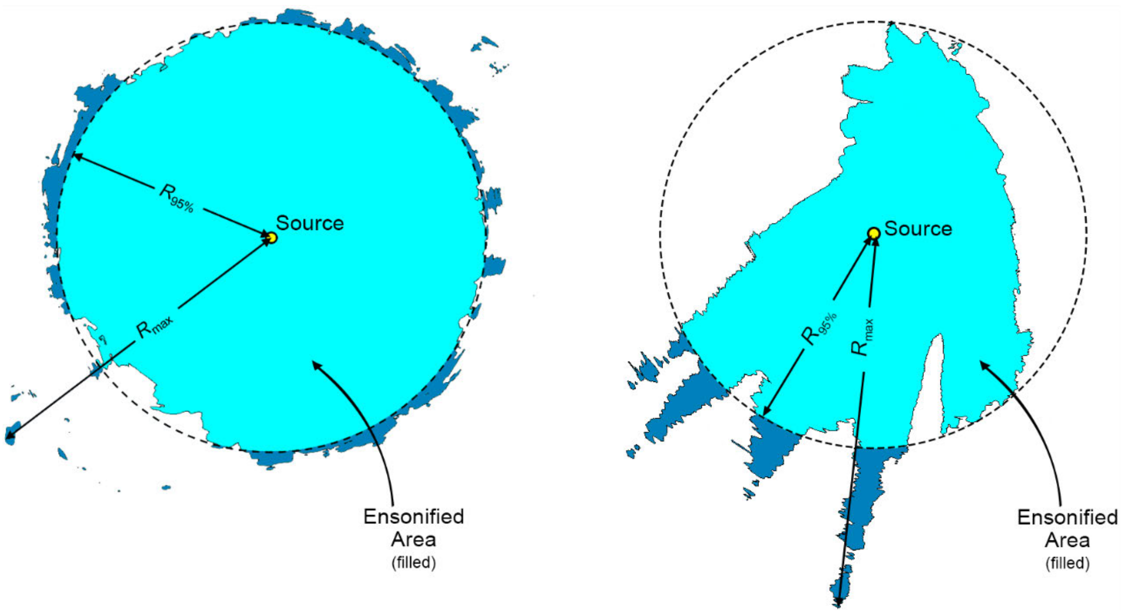

(a) (b)

Figure 2. Sample areas ensonified to an arbitrary sound level with R_{max} and $R_{95\%}$ ranges shown for two different scenarios. (a) Largely symmetric sound level contour with small protrusions. (b) Strongly asymmetric sound level contour with long protrusions. Light blue indicates the ensonified areas bounded by $R_{95\%}$; darker blue indicates the areas outside this boundary which determine R_{max}.

3. Results

This section presents acoustic contour maps that show the directivity and range to various sound level isopleths, and radii tables that contain the distances to injury and behavioural thresholds.

3.1. Sound Pressure Levels

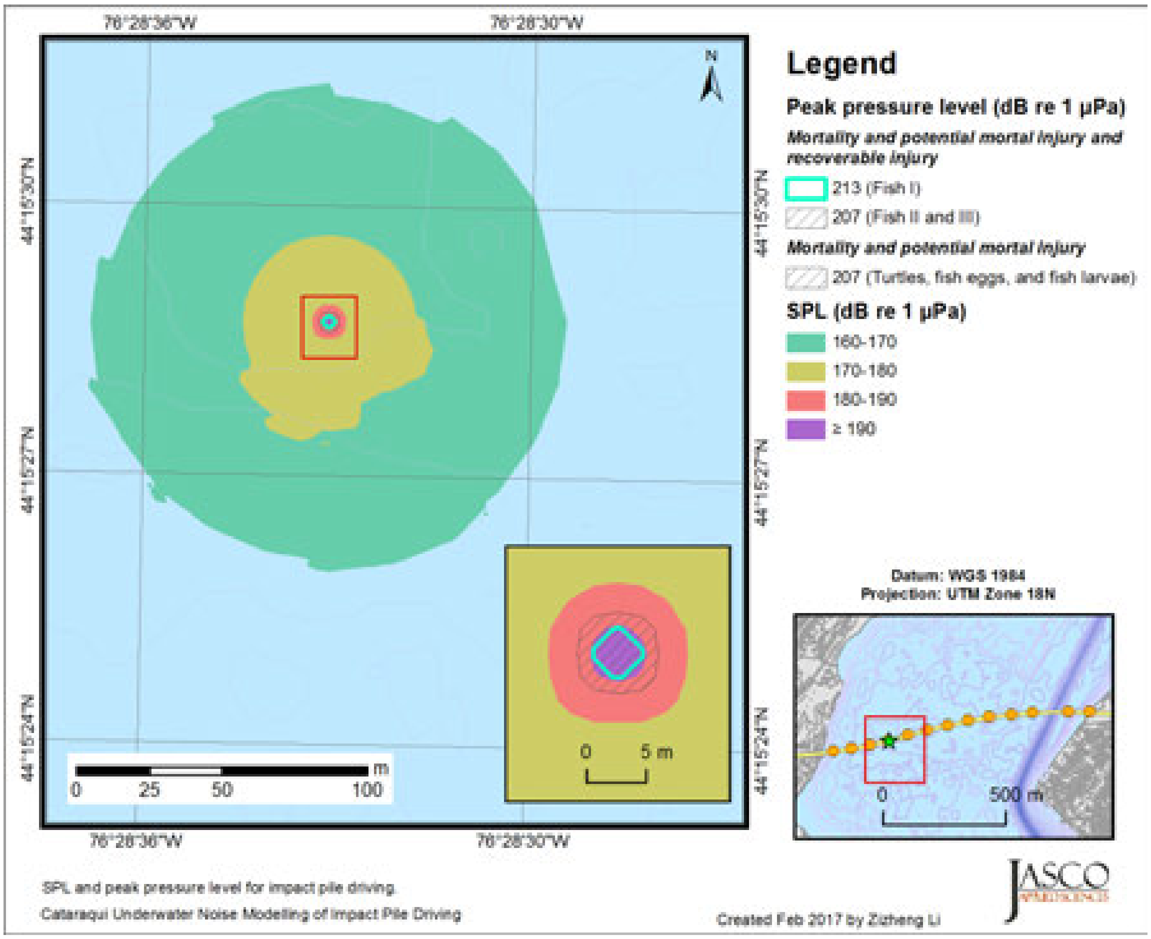

Figure 3. Maps of sound pressure level (SPL) and peak pressure level (PK) contours for impact pile driving without a bubble curtain.

Table 4. Distances (R_{max}, $R_{95\%}$) to PK and SPL contours from modelled impact pile driving without a bubble curtain. PK–peak pressure level; SPL–sound pressure level.

PK (dB re 1 µPa)	Distance (m)		SPL (dB re 1 µPa)	Distance (m)	
	R_{max}	$R_{95\%}$		R_{max}	$R_{95\%}$
220	-	-	190	2	2
210	3	3	180	6	6

PK (dB re 1 µPa)	Distance (m)		SPL (dB re 1 µPa)	Distance (m)	
	R_{max}	$R_{95\%}$		R_{max}	$R_{95\%}$
200	6	6	170	42	36
190	24	20	160	86	80

- indicates the level was not reached.

3.2. Sound Exposure Levels

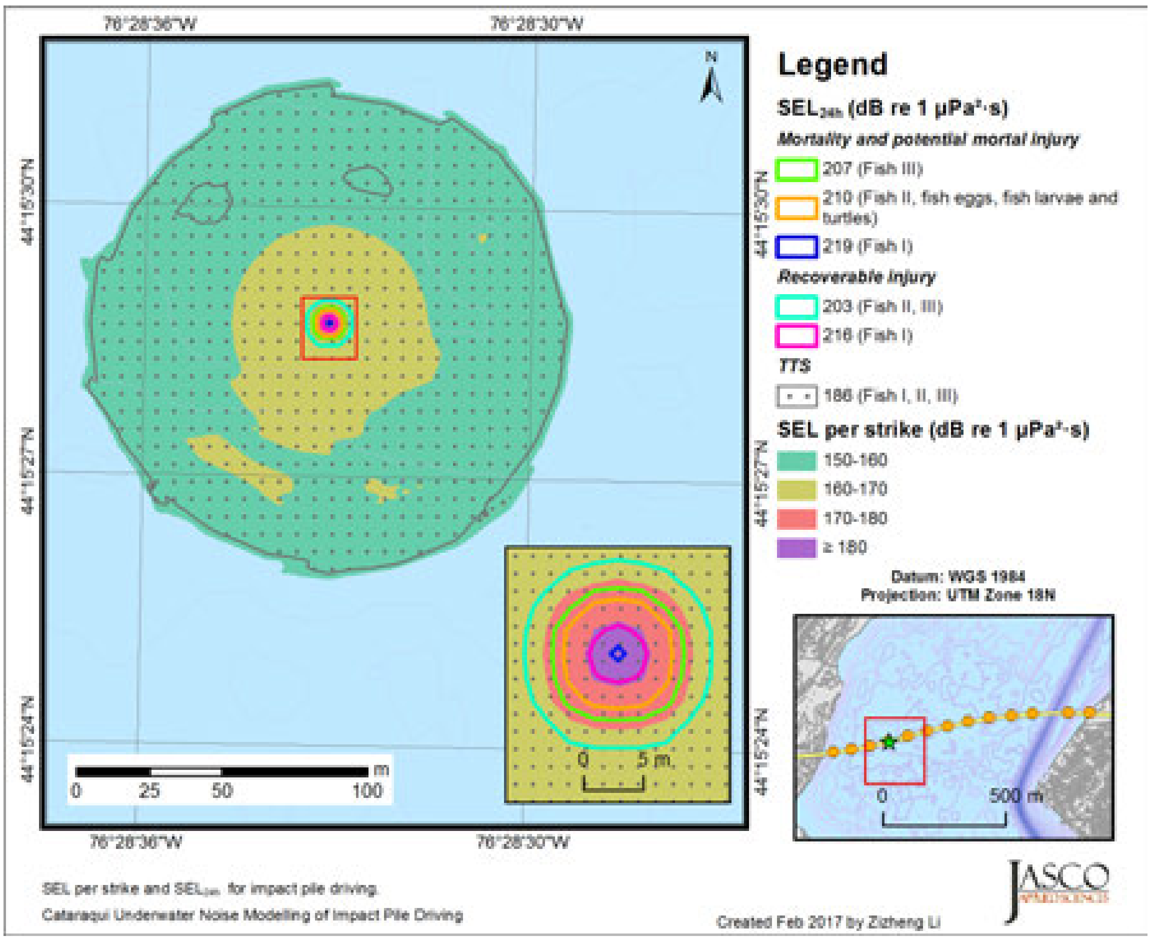

Figure 4. Maps of SEL per strike and SEL_{24h} contours for impact pile driving without a bubble curtain.

Table 5. Distances (R_{max}, $R_{95\%}$) to SEL per strike and SEL_{24h} contours from modelled impact pile driving without a bubble curtain. SEL–sound exposure level; SEL_{24h}–sound exposure level over 24 hours.

SEL per strike (dB re 1 µPa²·s)	Distance (m)		SEL_{24h} (dB re 1 µPa²·s)	Distance (m)	
	R_{max}	$R_{95\%}$		R_{max}	$R_{95\%}$
190	-	-	220	-	-
180	3	3	210	5	5
170	6	6	200	16	13
160	64	59	190	77	72

- indicates the level is not reached.

3.3. Distances to Criteria Thresholds

Table 6 summarizes the distances to thresholds proposed by Popper et al. (2014) (Section 1.3) for assessing possible effects on fish, turtles, fish eggs, and fish larvae. All of the fish in the area have swim bladders and many have additional adaptations that provide pressure sensitivity and extend the hearing frequency range (i.e., categories II and III). The maximum distance to thresholds for injury (including recoverable injury) for all fish was 7 m. The maximum distance for mortality or potential mortal injury to turtles, fish eggs, and fish larvae was 5 m. Quantitative thresholds for recoverable injury for turtles, fish eggs, or fish larvae are not specified by Popper et al. (2014). Likewise, Popper et al. (2014) do not suggest thresholds for masking or behavioral disruption in fish or turtles, but do indicate relative levels of risk as a function of range (Table 3).

Table 6. Distances (R_{max}, $R_{95\%}$) to injury thresholds for fish, fish eggs, fish larvae, and turtles (Popper et al. 2014) for impact pile driving without a bubble curtain. Fish I–No swim bladder; Fish II–Swim bladder not involved with hearing; Fish III–Swim bladder involved with hearing. PK–peak pressure level; SEL_{24h}–sound exposure level over 24 hours.

Type of animal	Threshold	Distance (m)	
		R_{max}	$R_{95\%}$
Mortality and potential mortal injury			
Fish I	213 dB re 1 µPa (PK)	2	2
Fish II, III, Fish eggs, Fish larvae, and Turtles	207 dB re 1 µPa (PK)	3	3
Fish I	219 dB re 1 µPa²·s (SEL_{24h})	-	-

Type of animal	Threshold	Distance (m)	
		R_{max}	$R_{95\%}$
Fish II, Fish eggs, Fish larvae, and Turtles	210 dB re 1 µPa²·s (SEL_{24h})	5	5
Fish III	207 dB re 1 µPa²·s (SEL_{24h})	6	6
Recoverable injury			
Fish I	213 dB re 1 µPa (PK)	2	2
Fish II, III	207 dB re 1 µPa (PK)	3	3
Fish I	216 dB re 1 µPa²·s (SEL_{24h})	2	2
Fish II, III	203 dB re 1 µPa²·s (SEL_{24h})	7	7
Temporary threshold shift			
Fish I, II, III	186 dB re 1 µPa²·s (SEL_{24h})	86	80

- indicate the level is not reached.

4. Discussion and Conclusion

4.1. Acoustic Modelling

This study used complementary models to estimate sound radiated into the environment by impact pile driving activities and propagation of sound through the water column and riverbed. Sound propagation was modelled in three dimensions (range, depth, and azimuth). The riverbed bathymetry and sub-bottom properties are the most important environmental factors governing propagation of sound from pile driving activities in this project. A portion of the sound generated by the driven pile is radiated directly into the riverbed, and in such a shallow environment there are multiple sound wave bottom interactions (i.e., bounces), thus transmission of sound into deeper sediment and rock layers and attenuation within the riverbed becomes significant loss factors for waterborne energy. At ranges of several water depths, which in this study is in a few meters, the absorption of sound energy into the riverbed (bottom loss) becomes the primary attenuation mechanism. The top sediment layer at the riverbed surface is composed of fine, water-saturated sediments (very loose silt, and silty clay to clay, Appendix B.3). In general, soft sediments allow for high penetration of acoustic energy and its subsequent attenuation as the acoustic wave propagates and interacts with sediments. A rocky bottom, by contrast, might be acoustically more reflective, returning more energy to the water column. Bottom loss is also affected by the stratification of the riverbed sediments, and is influenced by the frequency content of the sound. For example, low-frequency acoustic waves, which have long wavelengths, are not strongly affected by thin layers of sediment such as the top layer. Rather, low-frequency waves are likely to interact with deeper sediments and the bedrock, which generally possesses higher sound speeds and can reflect low-frequency energy back into the water column. Propagation at higher frequencies (i.e., short wavelengths) on the other hand, is characterized by shallower penetration and stronger interaction with the top soft sediment. Finally, interference between reflections from multiple sediment layers can enhance or suppress certain frequencies. Bottom loss, therefore, is a complex phenomenon.

To obtain reasonably precautionary noise levels, and so not underestimate potential effects on aquatic life, we made the following assumptions where uncertainties in operating conditions existed:

- The modelling location was selected because it had a thick layer of overburden which might require more strikes to set into bedrock, and is near the bird nesting wetland area to the north.
- All distances (R_{max}, $R_{95\%}$) and noise level contours represent the maximum sound levels over all modelled depths in the water column.
- The project schedule and operation plan were not finalized at the time of modelling. We have assumed each pile was installed by impact pile driving only, as it generates more underwater noise than either vibratory pile driving or rock socket drilling.

- Underwater vegetation is present throughout the water column in the river, which can play a role in scattering and attenuating sound. In this study, our sound propagation did not consider scattering effects due to underwater vegetation.

4.2. Impact to Animals

Based on the criteria proposed by Popper et al. (2014) for acoustic impacts on fish and turtles, the distances to the thresholds for injury are quite small (Table 6). The peak pressure thresholds for mortal and recoverable acoustic injury to fish and for mortal injury to fish eggs, fish larvae, and turtles occurred within 2–3 m of the source. The SEL_{24h} thresholds for mortal acoustic injury to fish with a swim bladder, fish eggs, fish larvae, and turtles were within 5–6 m of the source; the SEL_{24h} threshold for recoverable acoustic injury to fish with a swim bladder was within 7 m of the source. For dual-criteria thresholds, such as the peak pressure and SEL_{24h}, the greater of the two ranges is generally used for regulatory purposes. The maximum distance to the temporary threshold shift-onset (186 dB re 1 $\mu Pa^2 \cdot s$) was 86 m.

Popper et al. (2014) do not specify quantitative thresholds for recoverable injury for turtles, fish eggs, or fish larvae, nor do they specify quantitative thresholds for masking or behavioral disruption of any fish or turtle. Instead, qualitative risk levels as a function of relative range are used as shown in Table 3. Turtles within tens of meters of the pile are at high risk of recoverable injury, and fish eggs and larvae are at moderate risk of recoverable injury within this range. The relative risk drops to low for distances of hundreds to thousands of metres. Adult fish with a swim bladder not involved in hearing and turtles are at high risk of behavioural disruption within tens of metres of the pile, while fish with a swim bladder involved in hearing are at high risk within tens to hundreds of metres. Larval fish are at moderate risk of behavioural disturbance within tens of metres of the pile.

4.3. Mitigation System: Unconfined Bubble Curtain

As described in Section 2.2, bubble curtains are less effective when a significant portion of sound travels unimpeded through the sediment substrate and enters the water column via the bottom interface at a distance greater than the bubble curtain can contain. In this study, the pile is installed 45 m inside the riverbed sediments, and 0.54 m in the water column (water depth). Most of the sounds originated from and then travelled through the sediment substrate, refracting upwards towards the water column (Figure 5). In this case, the bubble curtain does not attenuate the sound propagation effectively. Based on our modelling results and due to such strong acoustic propagation within the sediment, the distances to thresholds using an unconfined bubble curtain are very similar to those without a bubble curtain. For a broader discussion of mitigation of underwater noise effects on wildlife, refer to the Third Crossing of the Cataraqui River Preliminary Design Natural Heritage Protection and Enhancement Plan (Golder 2017).

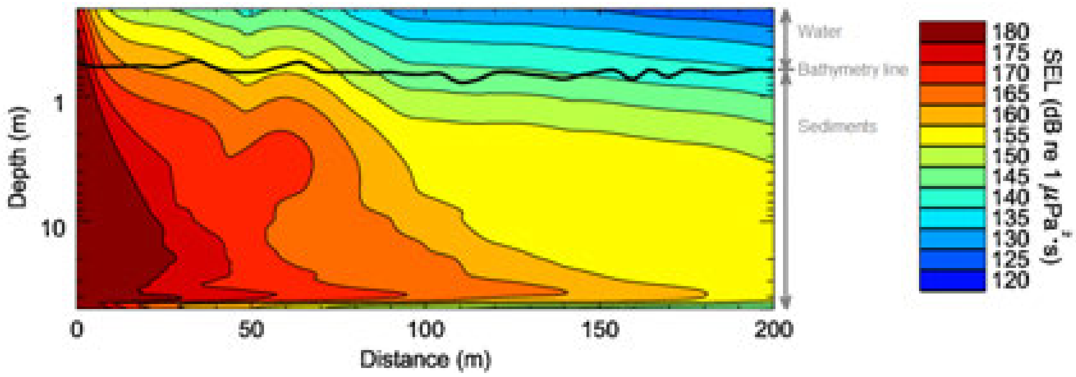

Figure 5. Sound exposure level (SEL) per strike along a northward radial from the modelling location showing the pile driving noise propagating through the riverbed sediment and water column.

Glossary

1/3-octave-band
Non-overlapping passbands that are one-third of an octave wide (where an octave is a doubling of frequency). Three adjacent 1/3-octave-bands comprise one octave. One-third-octave-bands become wider with increasing frequency. Also see octave.

absorption
The conversion of acoustic energy into heat, which is captured by insulation.

acoustic impedance
The ratio of the sound pressure in a medium to the rate of alternating flow of the medium through a specified surface due to the sound wave.

attenuation
The gradual loss of acoustic energy from absorption and scattering as sound propagates through a medium.

azimuth
A horizontal angle relative to a reference direction, which is often magnetic north or the direction of travel. In navigation it is also called bearing.

broadband sound level
The total sound pressure level measured over a specified frequency range. If the frequency range is unspecified, it refers to the entire measured frequency range.

compressional wave
A mechanical vibration wave in which the direction of particle motion is parallel to the direction of propagation. Also called primary wave or P-wave.

decibel (dB)
One-tenth of a bel. Unit of level when the base of the logarithm is the tenth root of ten, and the quantities concerned are proportional to power (ANSI S1.1-1994 R2004).

ensonified
Exposed to sound.

far-field
The zone where, to an observer, sound originating from an array of sources (or a spatially-distributed source) appears t o radiate from a single point. The distance to the acoustic far-field increases with frequency.

fast Fourier transform (FFT)
A computationally efficiently algorithm for computing the discrete Fourier transform.

frequency
The rate of oscillation of a periodic function measured in cycles-per-unit-time. The reciprocal of the period. Unit: hertz (Hz). Symbol: f. 1 Hz is equal to 1 cycle per second.

geoacoustic
Relating to the acoustic properties of the riverbed.

hertz (Hz)
A unit of frequency defined as one cycle per second.

intermittent sound
A level of sound that abruptly drops to the background noise level several times during the observation period.

impulsive sound
Sound that is typically brief and intermittent with rapid (within a few seconds) rise time and decay back to ambient levels (NOAA 2013, ANSI S12.7-1986 R2006). For example, seismic airguns and impact pile driving.

parabolic equation method
A computationally-efficient solution to the acoustic wave equation that is used to model transmission loss. The parabolic equation approximation omits effects of back-scattered sound, simplifying the computation of transmission loss. The effect of back-scattered sound is negligible for most ocean-acoustic propagation problems.

particle velocity
The physical speed of a particle in a material moving back and forth in the direction of the pressure wave. Unit: meters per second (m/s). Symbol: v.

peak pressure level (PK)
The maximum instantaneous sound pressure level, in a stated frequency band, within a stated period. Also called zero-to-peak pressure level. Unit: decibel (dB).

peak-to-peak pressure level
The difference between the maximum and minimum instantaneous pressure levels. Unit: decibel (dB).

percentile level, exceedance
The sound level exceeded n% of the time during a measurement.

permanent threshold shift (PTS)
A permanent loss of hearing sensitivity caused by excessive noise exposure. PTS is considered auditory injury.

point source
A source that radiates sound as if from a single point (ANSI S1.1-1994 R2004).

power spectrum density
The acoustic signal power per unit frequency as measured at a single frequency. Unit: μPa^2/Hz, or $\mu Pa^2 \cdot s$.

power spectral density level
The decibel level ($10\log_{10}$) of the power spectrum density, usually presented in 1 Hz bins. Unit: dB re 1 μPa^2/Hz.

pressure, acoustic
The deviation from the ambient hydrostatic pressure caused by a sound wave. Also called overpressure. Unit: pascal (Pa). Symbol: p.

pressure, hydrostatic
The pressure at any given depth in a static liquid that is the result of the weight of the liquid acting on a unit area at that depth, plus any pressure acting on the surface of the liquid. Unit: pascal (Pa).

received level
The sound level measured at a receiver.

rms
root-mean-square.

shear wave
A mechanical vibration wave in which the direction of particle motion is perpendicular to the direction of propagation. Also called secondary wave or S-wave. Shear waves propagate only in solid media, such as sediments or rock. Shear waves in the riverbed can be converted to compressional waves in water at the water-riverbed interface.

signature
Pressure signal generated by a source.

sound
A time-varying pressure disturbance generated by mechanical vibration waves travelling through a fluid medium such as air or water.

sound exposure
Time integral of squared, instantaneous frequency-weighted sound pressure over a stated time interval or event. Unit: pascal-squared second ($Pa^2 \cdot s$) (ANSI S1.1-1994 R2004).

sound exposure level (SEL)
A cumulative measure related to the sound energy in one or more pulses. Unit: dB re 1 $\mu Pa^2 \cdot s$. SEL is expressed over the summation period (e.g., per-pulse SEL [for airguns], single-strike SEL [for pile drivers], 24-hour SEL).

sound field
Region containing sound waves (ANSI S1.1-1994 R2004).

sound intensity
Sound energy flowing through a unit area perpendicular to the direction of propagation per unit time.

sound pressure level (SPL)
The decibel ratio of the time-mean-square sound pressure, in a stated frequency band, to the square of the reference sound pressure (ANSI S1.1-1994 R2004).

For sound in water, the reference sound pressure is one micropascal (p_0 = 1 μPa) and the unit for SPL is dB re 1 μPa:

$$\mathrm{SPL} = 10\log_{10}\left(p^2/p_0^2\right) = 20\log_{10}\left(p/p_0\right)$$

Unless otherwise stated, SPL refers to the root-mean-square sound pressure level. See also 90% sound pressure level.

sound speed profile
The speed of sound in the water column as a function of depth below the water surface.

source level (SL)
The sound level measured in the far-field and scaled back to a standard reference distance of 1 metre from the acoustic centre of the source. Unit: dB re 1 μPa @ 1 m (sound pressure level) or dB re 1 $\mu Pa^2 \cdot s$ (sound exposure level).

spectrum
An acoustic signal represented in terms of its power (or energy) distribution compared with frequency.

temporary threshold shift (TTS)
Temporary loss of hearing sensitivity caused by excessive noise exposure.

transmission loss (TL)
The decibel reduction in sound level between two stated points that results from sound spreading away from an acoustic source subject to the influence of the surrounding environment. Also called propagation loss.

wavelength
Distance over which a wave completes one oscillation cycle. Unit: meter (m). Symbol: λ.

Literature Cited

[NOAA] National Oceanic and Atmospheric Administration. 2013. Draft guidance for assessing the effects of anthropogenic sound on marine mammals: Acoustic threshold levels for onset of permanent and temporary threshold shifts, December 2013, 76 pp. Silver Spring, Maryland: NMFS Office of Protected Resources. http://www.nmfs.noaa.gov/pr/acoustics/draft_acoustic_guidance_2013.pdf.

[WSDOT] Washington State Department of Transportation. 2010. Underwater sound levels associated with driving steel piles for the State Route 520 bridge replacement and HOV project pile installation test program. Technical report prepared by Illingworth & Rodkin Inc. for Washington State Department of Transportation, Seattle WA.

ANSI S12.7-1986. R2006. American National Standard Methods for Measurements of Impulsive Noise. American National Standards Institute, New York.

ANSI S1.1-1994. R2004. American National Standard Acoustical Terminology. American National Standards Institute, New York.

Bartol, S.M., J.A. Musick, and M.L. Lenhardt. 1999. Auditory evoked potentials of the loggerhead sea turtle (Caretta caretta). Copeia: 836-840.

Bartol, S.M. and D.R. Ketten. 2006. Turtle and tuna hearing. In: Swimmer, Y. and R. Brill. Volume December 2006. NOAA Technical Memorandum NMFS-PIFSC-7. 98-103 pp. http://www.sefsc.noaa.gov/turtles/TM_NMFS_PIFSC_7_Swimmer_Brill.pdf#page=108.

Barton, N. 2007. Rock quality, seismic velocity, attenuation, and anisotropy. Taylor & Francis, Leiden, The Netherlands. 729

Bowfin Environmental Consulting. 2011. Proposed Third Crossing of the Cataraqui River – Environmental Assessment – Fisheries Results and Impact Analysis. City of Kingston Environmental Assessment, Third Crossing of the Cataraqui River. Prepared for J. L. Richards & Associates Ltd. 110 pp. https://www.cityofkingston.ca/documents/10180/45737/3RDX_EA-AquaticAnalysis.pdf/3b5d47ba-24d5-45a7-80e4-6435d2dd8166.

Bruintjes, R. and A.N. Radford. 2013. Context-dependent impacts of anthropogenic noise on individual and social behaviour in a cooperatively breeding fish. Animal Behaviour 85(6): 1343-1349. http://www.sciencedirect.com/science/article/pii/S0003347213001462.

Brumm, H. and H. Slabbekoorn. 2005. Acoustic Communication in Noise. In Peter J. B. Slater, Charles T. Snowdon, T.J. Roper, H.J. Brockmann, and N. Marc (eds.). Advances in the Study of Behavior. Volume 35. Academic Press. pp 151-209.

Buckingham, M.J. 2005. Compressional and shear wave properties of marine sediments: Comparisons between theory and data. Journal of the Acoustical Society of America 117(1): 137-152. http://link.aip.org/link/?JAS/117/137/1.

Codarin, A., L.E. Wysocki, F. Ladich, and M. Picciulin. 2009. Effects of ambient and boat noise on hearing and communication in three fish species living in a marine protected area (Miramare, Italy). Marine Pollution Bulletin 58(12): 1880-1887. http://www.sciencedirect.com/science/article/pii/S0025326X09003075.

Collins, M.D. 1993. A split-step Padé solution for the parabolic equation method. Journal of the Acoustical Society of America 93: 1736-1742.

De Robertis, A. and N.O. Handegard. 2013. Fish avoidance of research vessels and the efficacy of noise-reduced vessels: a review. ICES Journal of Marine Science: Journal du Conseil 70(1): 34-45. http://icesjms.oxfordjournals.org/content/70/1/34.abstract.

Fay, R.R. 1984. The goldfish ear codes the axis of acoustic particle motion in three dimensions. Science 225(4665): 951-954.

Fay, R.R. 1998. Hearing in vertebrates: A psychophysics databook. Hill-Fay Associates, Winnekta, IL.

Golder Associates Ltd. (Golder). 2017. Third Crossing of the Cataraqui River Preliminary Design Natural Heritage Protection and Enhancement Plan. Report No. 1541774. Prepared for J.L. Richards & Associates Ltd. and the City of Kingston.

Graham, A.L. and S.J. Cooke. 2008. The effects of noise disturbance from various recreational boating activities common to inland waters on the cardiac physiology of a freshwater fish, the largemouth bass (Micropterus salmoides). Aquatic Conservation: Marine and Freshwater Ecosystems 18(7): 1315-1324. http://dx.doi.org/10.1002/aqc.941.

Hastings, M.C. and A.N. Popper. 2005. Effects of sound on fish. In: Transportation, C.D.o. (ed.). Volume Contract 43A0139. http://www.dot.ca.gov/hq/env/bio/files/Effects_of_Sound_on_Fish23Aug05.pdf.

Kennedy, M. and M. Snow. 2016. Factual Data Report on: Preliminary Geotechnical Investigation Third Crossing of the Cataraqui River John Counter Boulevard to Gore Road Kingston, Ontario 1541774/2000/0003 DRAFT. Golder Associates report submitted to J.L. Richards & Associates Ltd. 151 pp.

Ketten, D.R., C. Merigo, E. Chiddick, H. Krum, and E.F. Melvin. 1999. Acoustic fatheads: parallel evolution of underwater sound reception mechanisms in dolphins, turtles, and sea birds. Journal of the Acoustical Society of America 105(2): 1110.

Ladich, F. and A.N. Popper. 2004. Parallel evolution in fish hearing organs. In Manley, G.A., A.N. Popper, and R.R. Fay (eds.). Evolution of the Vertebrate Auditory System Springer-Verlag, New York. pp 98-127.

Lavender, A.L., S.M. Bartol, and I.K. Bartol. 2012. Hearing capabilities of loggerhead sea turtles (Caretta caretta) throughout ontogeny. In The Effects of Noise on Aquatic Life. Springer. pp 89-92. http://www.soundandmarinelife.org/research-categories/physical-and-physiological-effects-and-hearing/modelling-mysticete-baleen-whale-hearing.aspx.

Lenhardt, M.L., R. Klinger, and J. Musick. 1985. Marine turtle middle-ear anatomy. Journal of Auditory Research 25(1): 66-72.

Lucke, K., P.A. Lepper, M.A. Blanchet, and U. Siebert. 2011. The use of an air bubble curtain to reduce the received sound levels for harbor porpoises (Phocoena phocoena). Journal of the Acoustical Society of America 130(5): 3406-3412.

MacGillivray, A. 2014. A model for underwater sound levels generated by marine impact pile driving. Proceedings of Meetings on Acoustics 20(1): 045008. http://scitation.aip.org/content/asa/journal/poma/20/1/10.1121/2.0000030.

MacGillivray, A.O. and N.R. Chapman. 2012. Modeling underwater sound propagation from an airgun array using the parabolic equation method. Canadian Acoustics 40(1): 19-25. http://jcaa.caa-aca.ca/index.php/jcaa/article/view/2502.

Marczak, W. 1997. Water as a standard in the measurements of speed in sound in liquids. Journal of the Acoustical Society of America: 2776-2779.

McCauley, R.D., J. Fewtrell, A.J. Duncan, C. Jenner, M.-N. Jenner, J.D. Penrose, R.I.T. Prince, A. Adihyta, J. Murdoch, et al. 2000. Marine seismic surveys: A study of environmental implications. Australian Petroleum Production Exploration Association (APPEA) Journal 40: 692-708.

Mitson, R.B. and H.P. Knudsen. 2003. Causes and effects of underwater noise on fish abundance estimation. Aquatic Living Resources 16(3): 255-263. http://www.sciencedirect.com/science/article/pii/S0990744003000214.

Moein, S.E., J.A. Musick, J.A. Keinath, D.E. Barnard, M.L. Lenhardt, and R. George. 1995. Evaluation of Seismic Sources for Repelling Sea Turtles from Hopper Dredges, in Sea Turtle Research Program: Summary Report. In: Hales, L.Z. (ed.). Report from U.S. Army Engineer Division, South Atlantic, Atlanta GA, and U.S. Naval Submarine Base, Kings Bay GA. Technical Report CERC-95. 90 pp.

Pile Dynamics, Inc. 2010. GRLWEAP.

Piniak, W.E., D.A. Mann, S.A. Eckert, and C.A. Harms. 2011. Amphibious hearing in sea turtles. In: Hawkins, T. and A.N. Popper (eds.). Proceedings of the 2nd International Conference on the Effects of Noise on Aquatic Life. August 15-20, 2010. Springer-Verlag. (In Press).

Plomp, R. and M.A. Bouman. 1959. Relation between Hearing Threshold and Duration for Tone Pulses. The Journal of the Acoustical Society of America 31(6): 749-758. http://scitation.aip.org/content/asa/journal/jasa/31/6/10.1121/1.1907781.

Popper, A.N., R.R. Fay, C. Platt, and O. Sand. 2003. Sound detection mechanisms and capabilities of teleost fishes. In Collin, S.P. and N.J. Marshall (eds.). Sensory processing in aquatic environments. Springer-Verlag, New York. pp 3-38.

Popper, A.N. and M.C. Hastings. 2009. The effects of anthropogenic sources of sound on fishes. Journal of Fish Biology 75: 455-489.

Popper, A.N., A.D. Hawkins, R.R. Fay, D.A. Mann, S. Bartol, T.J. Carlson, S. Coombs, W.T. Ellison, R.L. Gentry, et al. 2014. Sound Exposure Guidelines for Fishes and Sea Turtles: A Technical Report prepared by ANSI-Accredited Standards Committee S3/SC1 and registered with ANSI. SpringerBriefs in Oceanography, vol. ASA S3/SC1.4 TR-2014. ASA Press. 87 pp.

Ridgway, S.H., E.G. Wever, J.G. McCormick, J. Palin, and J.H. Anderson. 1969. Hearing in the giant sea turtle, Chelonia mydas. Proceedings of the National Academy of Sciences 64(3): 884-890.

Slabbekoorn, H., N. Bouton, I. van Opzeeland, A. Coers, C. ten Cate, and A.N. Popper. 2010. A noisy spring: The impact of globally rising underwater sound levels on fish. Trends in ecology & evolution (Personal edition) 25(7): 419-427. http://linkinghub.elsevier.com/retrieve/pii/S0169534710000832.

Smith, M.E., A.S. Kane, and A.N. Popper. 2004. Noise-induced stress response and hearing loss in goldfish (Carassius auratus). Journal of Experimental Biology 207(3): 427-435. http://jeb.biologists.org/content/207/3/427.abstract.

Vasconcelos, R.O., M.C.P. Amorim, and F. Ladich. 2007. Effects of ship noise on the detectability of communication signals in the Lusitanian toadfish. Journal of Experimental Biology 210(12): 2104-2112. http://jeb.biologists.org/content/210/12/2104.abstract.

Wever, E.G. 1978. The reptile ear: Its structure and function. Princeton University Press, Princeton, N.J.

Wysocki, L.E. and F. Ladich. 2005. Hearing in Fishes under Noise Conditions. Journal of the Association for Research in Otolaryngology 6(1): 28-36. http://dx.doi.org/10.1007/s10162-004-4043-4.

Wysocki, L.E., J.P. Dittami, and F. Ladich. 2006. Ship noise and cortisol secretion in European freshwater fishes. Biological Conservation 128(4): 501-508. http://www.sciencedirect.com/science/article/pii/S0006320705004350.

Zelick, R., D. Mann, and A.N. Popper. 1999. Acoustic communication in fishes and frogs. In Fay, R.R. and A.N. Popper (eds.). Comparative Hearing: Fish and Amphibians Springer-Verlag, New York. pp 363-411.

Zhang, Y. and C. Tindle. 1995. Improved equivalent fluid approximations for a low shear speed ocean bottom. Journal of the Acoustical Society of America 98(6): 3391-3396. http://scitation.aip.org/content/asa/journal/jasa/98/6/10.1121/1.413789.

Zykov, M.M., T.J. Deveau, and D. Zeddies. 2016. Modelling Underwater Sound Associated with Constructing Canaport Energy East Marine Terminal: Impact and Vibratory Pile Driving Noise. Document Number 01161, Version 3.0. Technical report by JASCO Applied Sciences for Stantec Consulting Ltd.

Appendix A. Underwater Acoustic Metrics

Underwater sound pressure amplitude is measured in decibels (dB) relative to a fixed reference pressure of p_0 = 1 μPa. Because the perceived loudness of sound, especially impulsive noise such as from seismic airguns, pile driving, and sonar, is not generally proportional to the instantaneous acoustic pressure, several sound level metrics are commonly used to evaluate noise and its effects on marine life. We provide specific definitions of relevant metrics used in the accompanying report. Where possible we follow the ANSI and ISO standard definitions and symbols for sound metrics, but these standards are not always consistent.

The zero-to-peak sound pressure level, or peak sound pressure level (PK; dB re 1 μPa), is the maximum instantaneous sound pressure level in a stated frequency band attained by an acoustic pressure signal, p(t):

$$L_{p,pk} = 20\log_{10}\left[\frac{\max(|p(t)|)}{p_0}\right] \quad \text{(A-1)}$$

$L_{p,pk}$ is often included as a criterion for assessing whether a sound is potentially injurious; however, because it does not account for the duration of a noise event, it is generally a poor indicator of perceived loudness.

The sound pressure level (SPL; dB re 1 μPa) is the rms pressure level in a stated frequency band over a specified time window (T, s) containing the acoustic event of interest. It is important to note that SPL always refers to an rms pressure level and therefore not instantaneous pressure:

$$L_p = 10\log_{10}\left(\frac{1}{T}\int_T p^2(t)dt \Big/ p_0^2\right) \quad \text{(A-2)}$$

The SPL represents a nominal effective continuous sound over the duration of an acoustic event, such as the emission of one acoustic pulse, a marine mammal vocalization, the passage of a vessel, or over a fixed duration. Because the window length, T, is the divisor, events with similar sound exposure level (SEL) but more spread out in time have a lower SPL.

The sound exposure level (SEL, dB re 1 μPa^2·s) is a measure related to the acoustic energy contained in one or more acoustic events (N). The SEL for a single event is computed from the time-integral of the squared pressure over the full event duration (T):

$$L_E = 10\log_{10}\left(\int_T p^2(t)dt \Big/ T_0 p_0^2\right) \quad \text{(A-3)}$$

where T_0 is a reference time interval of 1 s. The SEL continues to increase with time when non-zero pressure signals are present. It therefore can be construed as a dose-type measurement, so the integration time used must be carefully considered in terms of relevance for impact to the exposed recipients.

SEL can be calculated over periods with multiple acoustic events or over a fixed duration. For a fixed duration, the square pressure is integrated over the duration of interest. For multiple events, the SEL can be computed by summing (in linear units) the SEL of the N individual events:

$$L_{E,N} = 10\log_{10}\left(\sum_{i=1}^{N} 10^{\frac{L_{E,i}}{10}}\right) \quad \text{(A-4)}$$

For the SEL over 24 hours modelling scenario in this study, since SEL of each individual strike are assumed the same, the SEL can be computed by:

$$L_{E,N_{24h}} = L_E + 10\log_{10} N_{24h} \quad \text{(A-5)}$$

where L_E is per-strike SEL, and N_{24h} represents the total number of hammer strikes for impact pile driving over 24 hours.

Appendix B. Acoustic Environment

B.1. Bathymetry

FWRAM utilizes a high-resolution grid of bathymetry data to define water depths inside a region of interest. The water depth data provided by Golder Associates Ltd. were extracted and gridded onto a Universal Transverse Mercator (UTM) Zone 18 coordinate projection with a grid spacing of 5 m × 5 m (Figure B-1).

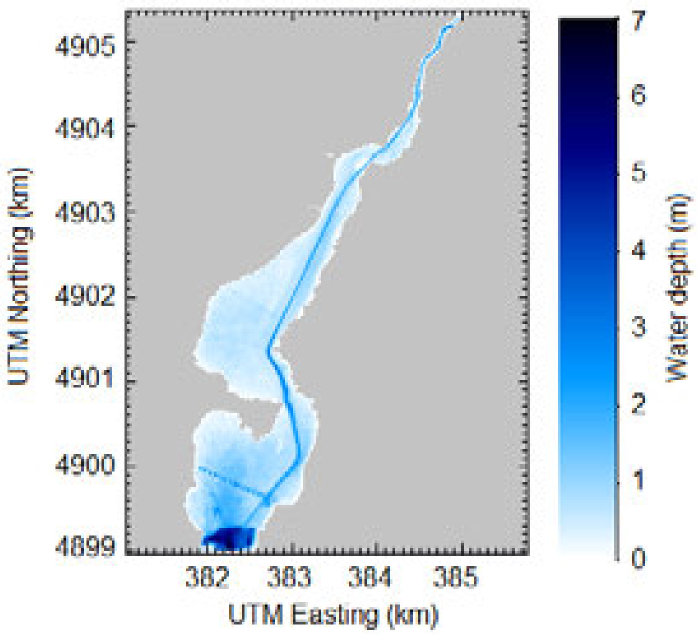

Figure B-1. Bathymetry grid used for acoustic modelling (UTM zone 18).

B.2. Water Sound Speed Profile

Temperature and salinity are the most important factors that determine the water sound speed profile (SSP). The salinity for freshwater is usually less that 0.5 ppt, which can be neglected in the SSP calculation. The SSP was thus computed directly from water temperature T (°C) using the formula of Marczak (1997):

$$c(T) = 1.402385\times10^{3} + 5.038813\mathrm{T} - 5.799136\times10^{-2}\mathrm{T}^{2} + 3.287156\times10^{-4}\mathrm{T}^{3} - 1.398845\times10^{-6}\mathrm{T}^{4} + 2.787860\times10^{-9}\mathrm{T}^{5} \quad \text{(B-1)}$$

It is currently anticipated that the impact pile driving will be carried out during the fall to minimize wildlife impacts. The water temperature was 7 °C for October (Bowfin Environmental Consulting 2011). Since the water depth is quite shallow in the study area (< 3 m in most of the area) and variation in temperature with depth is minimal, a uniform sound speed of 1434.9 m/s was taken to represent the mean sound speed conditions in Cataraqui River.

B.3. Geoacoustic Parameters

Sound propagation in shallow water is strongly influenced by the geoacoustic properties of the riverbed. These include the density, the compressional wave speed, the shear wave speed, the compressional wave attenuation, and the shear wave attenuation of the riverbed sediments.

The geoacoustic properties of the riverbed were estimated from geological stratigraphy data provided by Golder (Kennedy and Snow 2016). A cross-section of the riverbed stratigraphy was conducted at the Cataraqui bridge. Boreholes 16-103 and 16-104 were used to derive a general geoacoustic profile for the modelling area. The sediments at the bridge are composed primarily of very loose silt with organic matter, silty clay to clay with occasional very thin layers of silty clay and clayey silt, or clay, silt and fine sand, and gneiss bedrock. Descriptions of soil composition for these layers were used to estimate geoacoustic properties using the sediment grain-shearing model of Buckingham (2005). We based the sediment profile on the average and consistent features, i.e., a few meters of very loose silt over silty clay to clay. The geoacoustic properties for gneiss bedrock were obtained from Kennedy and Snow (2016) and Barton (2007). Table B-1 presents the geoacoustic parameters used for this study.

Table B-1. Geoacoustic parameters for the modelling area.Within each depth range, the parameters are increased linearly.

Depth below river floor (m)	Sediment Type	Density (g/cm^3)	Compressional wave speed (m/s)	Compressional wave attenuation (dB/λ)	Shear wave speed (m/s)	Shear wave attenuation (dB/λ)
0–3	Very loose silt	1.35	1420–1440	0.22–0.31	140	3.65
3–15	Silty clay to clay	1.35–1.56	1440–1490	0.31–0.52		
15–25		1.56–1.61	1490–1520	0.52–0.61		
25–43		1.61–1.69	1520–1560	0.61–0.70		
> 43	Bedrock	2.74	3500	0.10		

Appendix C. Sound and Hearing

C.1. Fish Hearing

Fish possess all of the basic acoustic processing capabilities of other vertebrates, including mammals (see review by Popper et al. 2003, Ladich and Popper 2004). Fish can discriminate between sounds of different magnitudes or frequencies, detect a sound in the presence of other signals, and determine the direction of a sound source.

Sound waves are characterized by compression and expansion of the medium as sound energy moves through it. This represents the pressure component of sound. At the same time, there is also back and forth motion of the particles making up the medium (particle motion). All fish directly sense the particle motion component of sound (Fay 1984), while relatively few fish also sense the pressure component (Popper et al. 2003). The ears of all fish consist of otolith- (or otoconia-) containing end organs that function as inertial accelerometers. Pressure-sensing fish have additional morphological adaptations that allow them to detect acoustic pressure (e.g., Popper et al. 2003). In these fish, gas-filled bladders near the ear (such as the swim bladder) or mechanical connections between the gas-filled bladder and the ear (e.g., Weberian ossicles) convey sound pressure from the water to the ear when the bladder deforms with pressure.

The majority of fish do not have specializations for sensing pressure; they detect only particle motion and their hearing frequency range is typically limited to frequencies below 1 kHz. Pressure-sensing fish tend to have extended hearing bandwidth and lower detection thresholds. They are often capable of detecting signals up to 3–4 kHz with thresholds may be 20 dB or more lower than the pressure-insensitive fish (Hastings and Popper 2005). Pressure sensitivity is not strictly related to fish taxonomy as pressure sensing occurs in several fish taxonomic groups. Hearing abilities have been determined for relatively few (~100) of the more than 27,000 extant fish species (see Fay 1998, Popper et al. 2003). Hearing capabilities between different species, especially those that are taxonomically or geographically distant, must be extrapolated with caution.

C.2. Potential Effects of Sound on Fish

Fish use sounds in a wide variety of behaviours including aggression, territory protection, defense, and reproduction (reviewed by Zelick et al. 1999). The presence of anthropogenic sounds could reduce the ability of fish to detect and characterize important signals (Slabbekoorn et al. 2010). If anthropogenic noise deters fish, or if noise negatively affects fish survival and reproduction, a likely result would be decreased fish diversity and density at noisy sites (Slabbekoorn et al. 2010). Few studies have been conducted to evaluate such negative correlations between the presence of fish and the presence of noise, though some studies report an effect of vessel noise on fish flight behaviour in the context of population assessments and catch rates for commercially important fish stocks (reviewed by Mitson and Knudsen 2003, De Robertis and Handegard 2013).

Several studies on captive fish have shown that fish exposed to simulated boat noise increase secretion of the stress hormone cortisol (Smith et al. 2004, Wysocki et al. 2006), exhibit an increase in heart rate (Graham and Cooke 2008), and can experience hearing damage (Smith et al. 2004). Behavioural changes have also been observed (e.g., Bruintjes and Radford 2013). Because fish produce low frequency sounds to communicate during reproduction, the presence of anthropogenic noise could prevent fish from detecting and recognizing one another (Brumm and Slabbekoorn 2005, Wysocki and Ladich 2005, Vasconcelos et al. 2007, Codarin et al. 2009), resulting in decreased reproductive success. Potential adverse effects of noise on fish hearing, have been measured in laboratories and in the field (see review by Popper and Hastings 2009), although many noise sources have not been studied. Because hearing abilities differ between fish species, the effect of anthropogenic noise may vary considerably.

C.3. Turtle Hearing

There is little information on turtle hearing. Morphological studies of green and loggerhead sea turtles (Ridgway et al. 1969, Wever 1978, Lenhardt et al. 1985) find that the sea turtle ear is similar to other reptile ears, but has some adaptations for underwater listening. A thick layer of fat may conduct sound to the ear in a similar manner as the fat in jawbones of odontocetes (Ketten et al. 1999), but sea turtles also have an air cavity that presumably increases sensitivity to sound pressure. Electrophysiological and behavioural studies on green and loggerhead sea turtles found their hearing frequency range is ~50–2000 Hz (Ridgway et al. 1969, Bartol et al. 1999, Bartol and Ketten 2006, Piniak et al. 2011, Lavender et al. 2012). No information is available on underwater hearing in freshwater turtles.

C.4. Potential Effects of Sound on Turtles

There are few data about the response of turtles to acoustic exposure, and there are no studies of hearing loss or the effects of exposure to loud sounds. McCauley et al. (2000) reports the behavioural response of caged green and loggerhead turtles to an approaching seismic airgun—for received levels above SPL 166 dB re 1 µPa the turtles increased their swimming activity and above SPL 175 dB re 1 µPa they began to behave erratically, which was interpreted as an agitated state. Additional data suggest that behavioural responses occur closer to SPL 175 dB re 1 µPa and TTS or PTS occur at even higher levels (Moein et al. 1995).

Appendix D. Pile Driving Source Model

A physical model of pile vibration and near-field sound radiation is used to calculate source levels of piles. The physical model employed in this study computes the underwater vibration and sound radiation of a pile by solving the theoretical equations of motion for axial and radial vibrations of a cylindrical shell. These equations of motion are solved subject to boundary conditions, which describe the forcing function of the hammer at the top of the pile and the soil resistance at the base of the pile (Figure D-1). Damping of the pile vibration due to radiation loading is computed for Mach waves emanating from the pile wall. The equations of motion are discretised using the finite difference (FD) method and are solved on a discrete time and depth mesh.

To model the sound emissions from the piles, the force of the pile driving hammers also had to be modelled. The force at the top of each pile was computed using the GRLWEAP 2010 wave equation model (GRLWEAP, Pile Dynamics 2010), which includes a large database of simulated hammers—both impact and vibratory—based on the manufacturer's specifications. The forcing functions from GRLWEAP were used as inputs to the FD model to compute the resulting pile vibrations.

The sound radiating from the pile itself is simulated using a vertical array of discrete point sources. The point sources are centred on the pile axis. Their amplitudes are derived using an inverse technique, such that their collective particle velocity—calculated using a near-field wave-number integration model—matches the particle velocity in the water at the pile wall. The sound field propagating away from the vertical source array is then calculated using a time-domain acoustic propagation model (Appendix E). MacGillivray (2014) describes the theory behind the physical model in more detail.

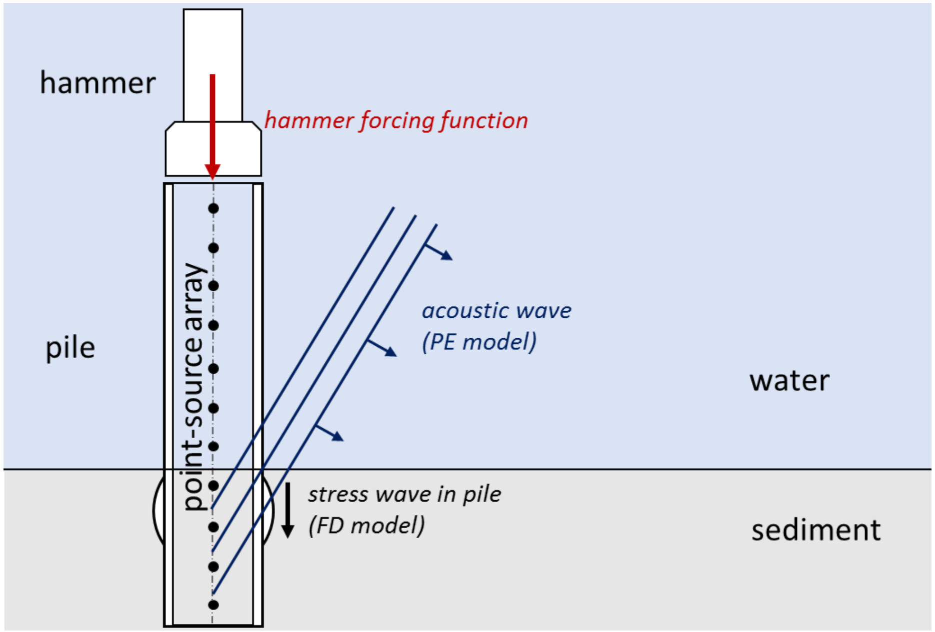

Figure D-1. Physical model geometry for impact driving of a cylindrical pile (vertical cross-section). The hammer forcing function is used with the finite difference (FD) model to compute the stress wave vibration in the pile. A vertical array of point sources is used with the parabolic equation (PE) model to compute the acoustic waves that the pile wall radiates.

In this study, based on the parameters described in Section 2.1, the force at the top of the pile generated by the driver (Figure D-2) was computed using the GRLWEAP 2010 wave equation model and input to PDSM. The forcing function for the hammer was modelled assuming that driving was carried out using the maximum recommended hammer energy. The finite difference (FD) model was then used to compute the resulting pile vibrations (Figure D-3). The stress wave reflection coefficient at the pile tip was assumed to be −0.5, which yielded a vertical pile displacements of 25 mm/strike for the 335 kJ hammer, consistent with estimates from the driveability analysis. Pressure signatures for the point-sources were computed from the particle velocity at the pile wall up to a maximum frequency of 1024 Hz. This frequency range was deemed suitable, since the majority of the sound energy generated by the piles was below 1 kHz (Figure D-4). The pile was represented as 500 discrete point-sources, evenly distributed over the length of the pile with a vertical separation of 0.1 m. The acoustic energy at higher frequencies (1–4 kHz) was extrapolated using a −2 dB per 1/3-octave-band roll-off coefficient (Section 2.2).

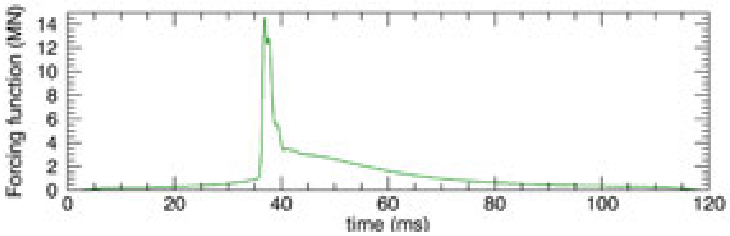

Figure D-2. Modelled forcing function versus time for the APE D100-42 diesel impact hammer for 42-inch steel cylindrical pipe piles.

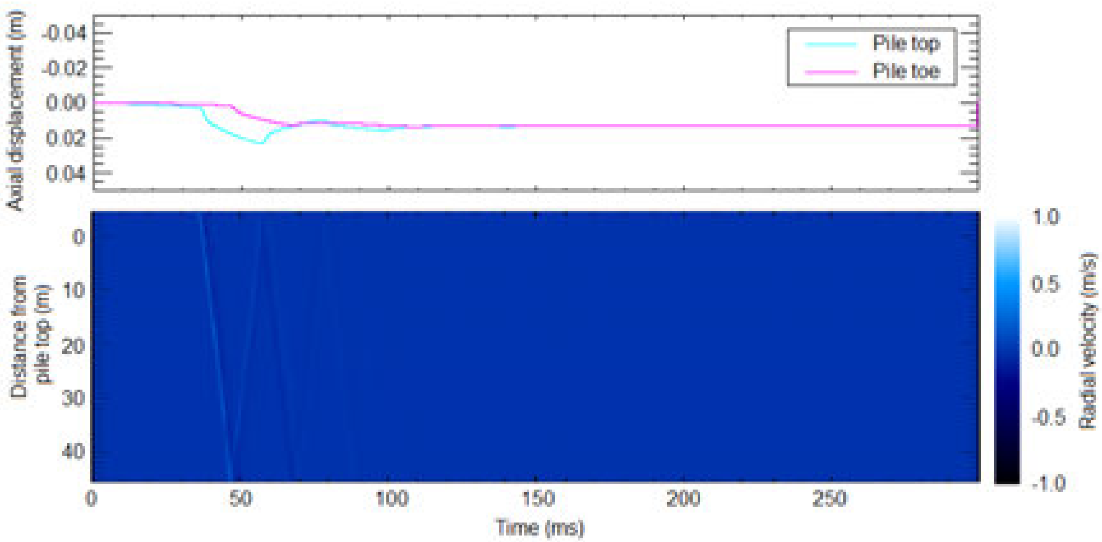

Figure D-3. vertical displacement (top) and radial wall velocity (bottom) as computed by the finite difference model.

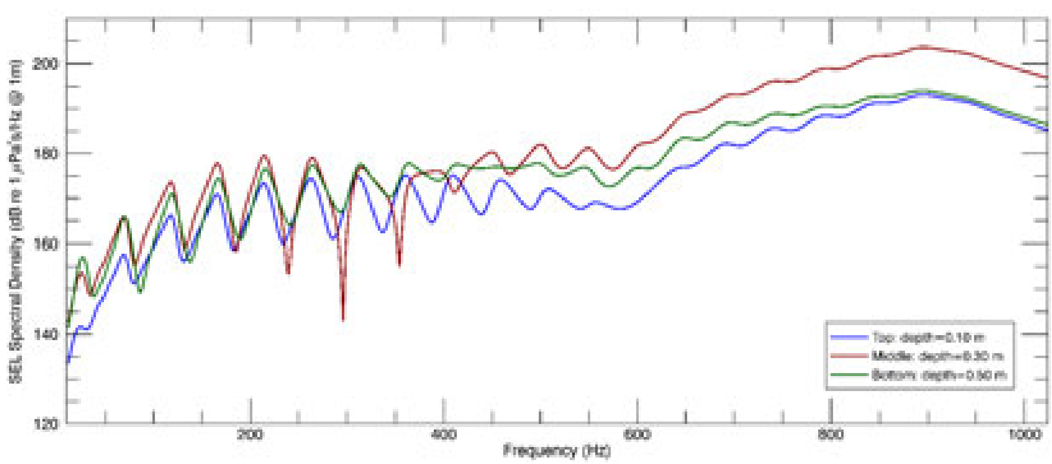

Figure D-4. SEL spectral density of acoustic point sources calculated by the finite difference (FD) model. Spectra are shown for the top, middle, and bottom of the pile in the water column.

Appendix E. Full Waveform Range-dependent Acoustic Model (FWRAM)

For impulsive sounds from impact pile driving, time-domain representations of the pressure waves generated in the water are required to calculate SPL and peak pressure level. Furthermore, the pile must be represented as a distributed source to accurately characterise vertical directivity effects in the near-field zone. For this study, synthetic pressure waveforms were computed using FWRAM, which is a time-domain acoustic model based on a version of the U.S. Naval Research Laboratory's Range-dependent Acoustic Model (RAM), which has been modified to account for a solid seabed (Zhang and Tindle 1995). FWRAM computes synthetic pressure waveforms versus range and depth for range-varying marine acoustic environments. FWRAM incorporates the following site-specific environmental properties: a bathymetric grid of the modelled area, underwater sound speed as a function of depth, and a geoacoustic profile based on the overall stratified composition of the riverbed. FWRAM computes pressure waveforms via Fourier synthesis of the modelled acoustic transfer function in closely spaced frequency bands. It employs the array starter method to accurately model sound propagation from a spatially distributed source (MacGillivray and Chapman 2012).

Synthetic pressure waveforms were modelled over the frequency range 10–1024 Hz, inside a 1 s window (Figure E-1). The synthetic pressure waveforms were post-processed, after applying a travel time correction, to calculate standard SPL and SEL metrics versus range and depth from the source. Figure E-2 shows the received levels (PK, SPL, and SEL per strike) along that 45° radial that extended to 1 km.

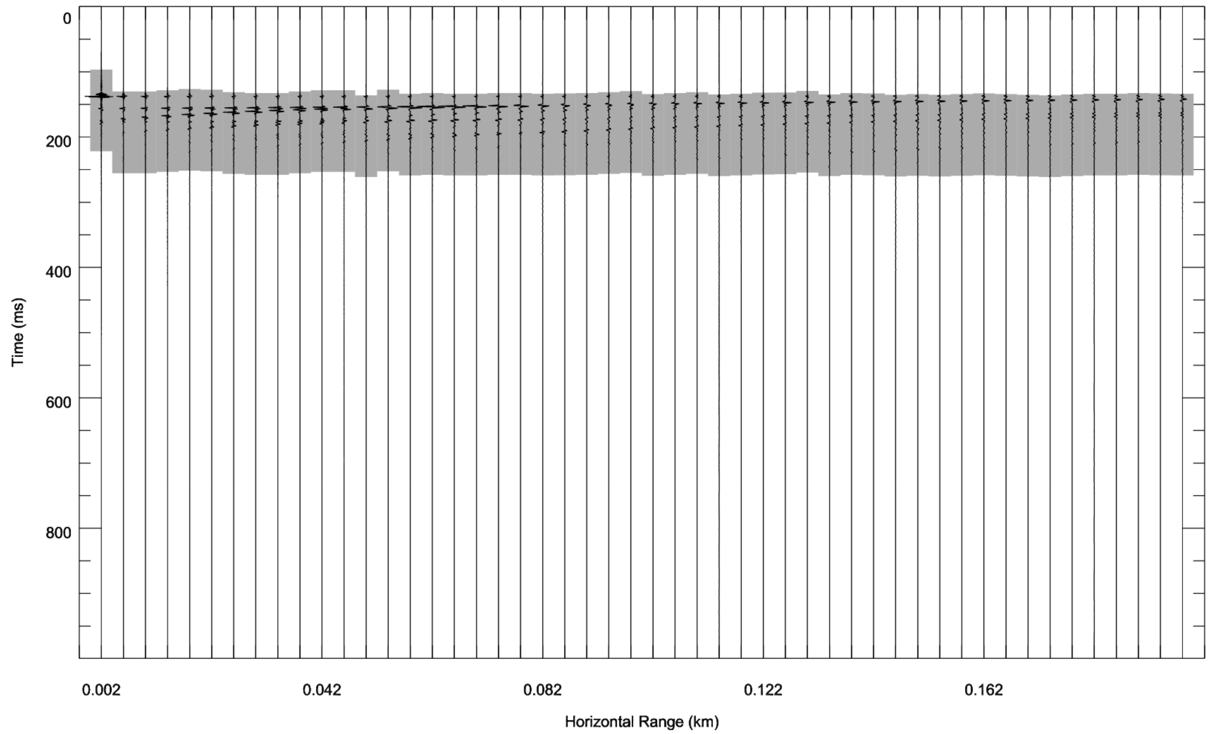

Figure E-1. Synthetic pressure waveforms computed by FWRAM for a modelled radial. The radial azimuth angle is 45° with range step size of 2 m. The gray shades indicate the integrated time to compute sound pressure level.

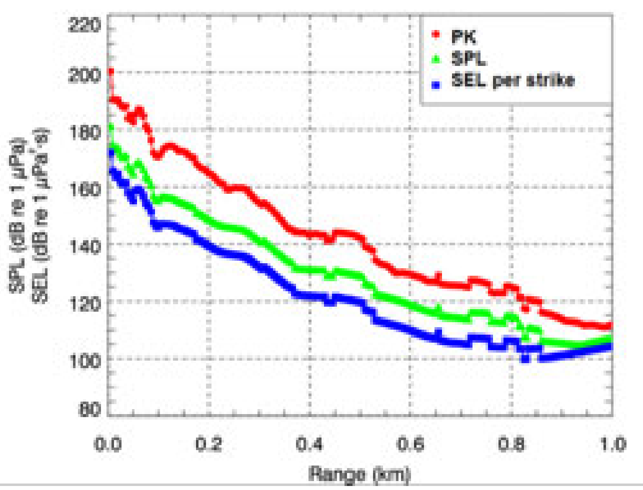

Figure E-2. Peak pressure level (PK), sound pressure level (SPL) and sound exposure level (SEL) per strike as a function of range along one modeled radial. The radial azimuth angle is 45° and extended to 1 km.